



Journal of Agrometeorology

(A publication of Association of Agrometeorologists)

ISSN : 0972-1665 (print), 2583-2980 (online)

Vol. No. 27 (4) : 494-502 (December - 2025)

<https://doi.org/10.54386/jam.v27i4.3178>

<https://journal.agrimetassociation.org/index.php/jam>



Research Paper

A study on vertical profiling of air pollutants and meteorological variables in Visakhapatnam, an Indian coastal urban environment

PRIYANKA PRIYADARSHINI NYAYAPATHI, SRINIVAS NAMUDURI, and SURESH KUMAR KOLLI*

Department of Life Sciences – Environmental Science Division, School of Science, GITAM Deemed to be University, Visakhapatnam, Andhra Pradesh, India

*Corresponding author: skolli@gitam.edu

ABSTRACT

Air pollution in coastal urban environments is a complex interplay of emission sources and meteorological conditions, often inadequately captured by traditional horizontal monitoring. This study investigates the vertical distribution of major air pollutants $PM_{2.5}$, PM_{10} , SO_2 , NO_2 , NO and CO across five high-rise multi-storey buildings in Rushikonda, Visakhapatnam, during summer and winter seasons. Over 30 days of continuous monitoring with a distinct vertical gradient, where noticeable variations were observed, particularly for particulate matter, with $PM_{2.5}$ and PM_{10} concentrations decreasing by up to 10.2% and 15.4%, respectively, from ground to elevated levels. However, statistical data analysis and 3-D visualization of the relationship between the pollutants and the meteorological parameters revealed critical thresholds for temperature, relative humidity (RH), and height influencing pollutant stratification. 3D surface visualizations further emphasized RH's role in enhancing particulate concentrations via hygroscopic growth and suppressing vertical dispersion, besides the long-range transport of air mass could also contribute to the high concentration values of particulate matter. The findings highlight the utility of vertical monitoring using existing urban infrastructure and underscore its relevance in refining air quality management in coastal cities.

Keywords: Urban environment, Vertical distribution, Air quality monitoring, Air pollutants, Relative humidity, Temperature

Air pollution is one of the most pressing environmental challenges, ranking as a leading cause of preventable morbidity and mortality worldwide. In many cases, air pollution is often more severe in urban areas since they are commonly accompanied by larger concentrations of anthropogenic sources. The developing countries like India, predominantly face the dire situation where air pollution is accountably responsible for over a million premature deaths per year, owing to cardiovascular diseases, chronic obstructive pulmonary diseases (COPD), lung cancer and acute respiratory infections (Gupta and Kumar, 2023). The prime pollutants contributing to such crisis include fine particulate matter ($PM_{2.5}$ and PM_{10}), nitrogen dioxide (NO_2), sulphur dioxide (SO_2), ozone(O_3), and carbon monoxide (CO). Among these, the particulate matter stands out as the principal atmospheric pollutant driving a significant threat to human and climatic health. Owing to their tiny size, comparable to the wavelength of visible light, these particles can have a stronger impact on atmospheric conditions than larger pollutants (Meo *et al.*, 2024).

PM in the atmosphere originates from diverse sources, including coal combustion, vehicular emissions, industrial discharges, dust resuspension, and biomass burning. While the complete eradication of PM sources is impractical, significant reductions are achievable through stringent policy interventions and advancements in pollution control technologies (Jalali *et al.*, 2022). However, due to funding restrictions and technical limitations, most of the current methodologies predominantly focusing on two-dimensional horizontal profiling, thereby neglecting the vertical stratification of pollutants. This gap in the research restricts our understanding of how air pollution disperses, particularly in relation to large scale atmospheric movement and long-range transport of pollutants. In addition, in South Korea, where research has shown that pollution carried over long range transport contributes to 19% of PM_{10} and a staggering 38.4% of $PM_{2.5}$ concentrations. Since air pollution can travel hundreds and even thousands of meters above the ground, studying its vertical distribution is critical for effective pollution control and regional cooperation on air quality management.

Article info - DOI: <https://doi.org/10.54386/jam.v27i4.3178>

Received: 2 September 2025; Accepted: 22 September 2025; Published online : 1 December 2025

"This work is licensed under Creative Common Attribution-Non Commercial-ShareAlike 4.0 International (CC BY-NC-SA 4.0) © Author (s)"

The vertical distribution of atmospheric pollutants has been studied using various methods, including aircraft, high-rise buildings/meteorological towers, remote sensing, tethered balloons, and unmanned aerial vehicles (UAVs), each offering distinct advantages and limitations for environmental monitoring. High-rise monitoring enables continuous, long-term data collection with fine vertical resolution, surpassing the intermittent nature of airborne or remote sensing methods. The studies using the Beijing Meteorological Tower have demonstrated how vertical air pollution and meteorological data can be captured across multiple layers of the atmosphere, offering insights into pollutant stratification and boundary layer dynamics (Zhao *et al.*, 2022). This technique requires lesser installation costs for researchers to capture concentrations of pollutants at different altitudes on dedicated instrument platforms. Pollutants from various sources continuously interact within the boundary layer of the atmosphere, making it important to track their vertical dispersion. However, the planetary boundary layer (PBL) stability due to wind speed and solar radiation affects the dust and pollutant dispersion, thereby exacerbating the urban air pollution levels. Therefore, by leveraging high-rise structures, researchers can gain insights into these processes so that the management of air quality can be done better.

The present study aims to study the vertical distribution of major pollutants ($PM_{2.5}$ and PM_{10} , CO, SO_2 , NO and NO_2) with respect to meteorological factors. Although the windspeed serves a prime role in pollutant dispersion, it was not included in the study due to its defined scope and boundaries of current research, thereby acknowledging it as a limitation. Our study focuses on the significant part played by temperature and relative humidity in influencing the spatial pattern of pollutants. This will further enhance our understanding of the dynamic spatial distribution of air pollutants on the local scale.

MATERIALS AND METHODS

Site description and experiment design

Rushikonda, a coastal region in Vishakhapatnam along the eastern coast of India, experiences a tropical climate characterized by hot summers, moderate winters, and significant rainfall. This region is distinguished by its unique geographical and environmental features, making it a crucial site for atmospheric studies. Within this area, GITAM Deemed to be a university serves as a strategically significant location for air quality monitoring due to its proximity to urban centres, small-scale industries, and marine environments. The site is influenced by diverse emission sources, including vehicular traffic, marine aerosols and construction dust, making it an ideal setting to investigate the interaction of atmospheric pollutants with coastal meteorology. Given its close proximity to the coastline, GITAM experiences fair humidity levels, which facilitate the transport of dust particles as moisture laden air can act as a carrier for particulate matter. Considering these factors, the study was conducted at GITAM ($17^{\circ} 46' 53.1192''$ N, $83^{\circ} 22' 35.8536''$ E) as shown in Fig. 1, to assess the vertical distribution of air pollutants.

Measurement technique and methodology

Monitoring was conducted at five different locations

within the study site during two distinct seasonal periods: from March 4th to March 25th of 2024, representing summer, and from December 2nd to December 23rd of 2024, representing winter, based on the CPCB classification of seasons. The study encompassed varying building heights, with the highest altitude reaching 50 meters. Monitoring stations at each location were established at intervals of 10 meters in height. However, due to differences in building elevations, the number of monitoring points varied across locations: at Pharmacy building (L1) and CV Raman Bhavan (L2), where buildings were of equal height, measurements were taken at three levels; at Sadarama Sadan (L3) four levels were considered; at ICT building (L4) five levels were included; and at Deshmukh Sadan (L5) six levels were monitored at 10 metre interval heights. The monitoring process followed a structured rotational schedule. Each day, starting from March 4th, measurements were taken at a specific location, beginning with location L1, where three monitoring instruments were installed at different heights and continuously recorded data for eight hours, from 8:00 AM to 4:00 PM. On March 5th, the same process was repeated at location L2, and so forth, completing one full rotation across all locations. This cycle was repeated twice more, ensuring comprehensive data collection until March 25th. A similar approach was adopted during the winter monitoring phase from December 2nd to December 23rd. Given that the highest building in the study area reached 50 meters, six monitoring instruments were deployed accordingly to capture variations in air quality parameters across different heights. The placement of these instruments was determined based on the specific requirements of the study to ensure accurate and representative data collection. Data collection was carried out over a period of 30 days, allowing for an in-depth analysis of how meteorological parameters influence pollutant dispersion at varying altitudes.

Real time ambient air quality monitoring

The present study primarily focuses on the vertical measurement of atmospheric pollutants using a sensor-based Mini Ambient Air Quality Monitoring System (Mini AAQMS) that has been developed by Swan as a multipurpose scientific platform, as shown in Fig. 2. To maintain a system with high availability, Mini AAQMS was developed by integrating sophisticated dual-sensor technology. As for particulate matter (PM_{10} and $PM_{2.5}$) measurements, the system employs the 90° light scattering technique, with the measurement range of 0 to 30,000 $mg\ m^{-3}$ with the resolution of 1 $mg\ m^{-3}$. The equipment with electrochemical sensors uses carbon monoxide (CO), sulphur dioxide (SO_2), nitric oxide (NO), and nitrogen dioxide (NO_2) sensors to detect gaseous measurements. In accordance with the CPCB guidelines, the most effective approach, which combines both sensor-controlled detection and manual monitoring, was adopted. This helped to increase the accuracy of the collected data, as well as achieve the goals of the National Ambient Air Quality Standards (NAAQS). The automation protocol was implemented with the APM 550 Fine Particulate Sampler and the APM 460 Respirable Dust Sampler. The APM 550, designed for the collection of $PM_{2.5}$, employs a battery of multi-stage impactors in order to comply with the USEPA standards. This APM 460 works at the air flow rate of 0.9 to 1.4 $m^3\ min^{-1}$ and it kind of works as a pre-separator for the harder particles up to 10 microns. The consistent deployment of APM 550 and APM 460 enables to have a synergistic



Fig. 1: Sampling locations in Visakhapatnam, India

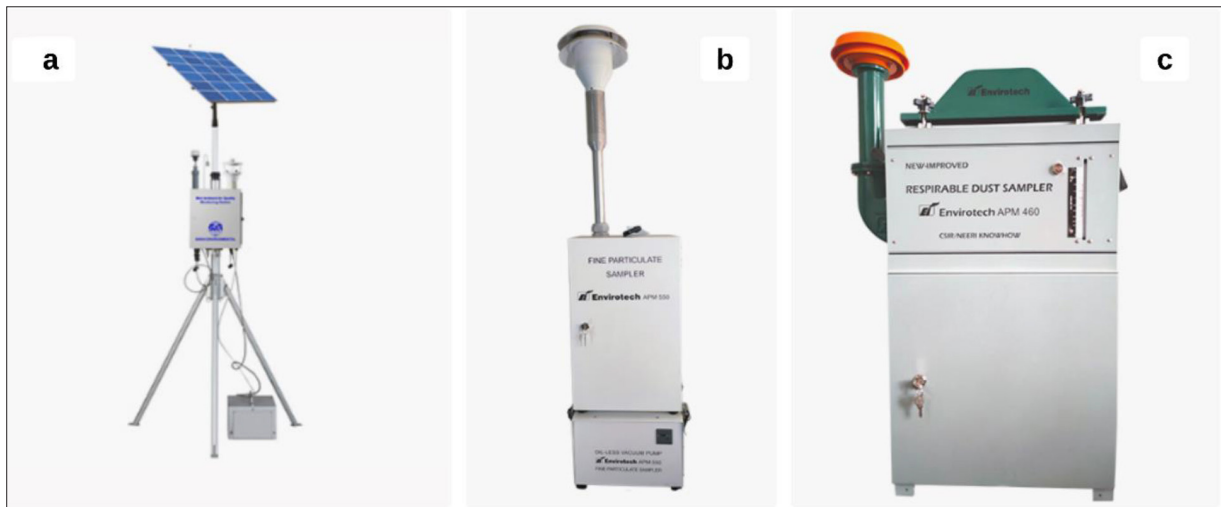


Fig. 2: Ambient air quality monitoring: (a) Sensor-based mini ambient air quality monitoring system (Mini AAQMS), (b) APM 550 fine particulate sampler, and (c) APM 460 respirable dust sampler

and comprehensive monitoring approach, thereby providing robust data on the PM distribution. The involvement of advanced design features ensures operational resilience, accuracy, and adaptability across diverse environmental conditions, thereby supporting high-quality environmental monitoring.

RESULTS AND DISCUSSION

Data analysis

The statistical summary of pollutant concentrations across the five monitoring locations has revealed distinct spatial variations,

Table 1: Mean and standard deviation (\pm SD) of pollutant concentrations across the monitoring locations

Pollutants	Pharmacy building (L1)	CV Raman Bhavan (L2)	Sadarama Sadan (L3)	ICT building (L4)	Deshmukh Sadan (L5)
PM ₁₀	97.29 \pm 13.30	99.08 \pm 18.32	96.66 \pm 22.58	96.23 \pm 22.31	91.65 \pm 43.43
PM _{2.5}	82.52 \pm 17.87	88.73 \pm 7.49	115.98 \pm 26.74	74.70 \pm 15.05	98.09 \pm 24.48
SO ₂	68.54 \pm 6.90	70.09 \pm 6.24	65.47 \pm 6.27	66.46 \pm 5.98	64.04 \pm 5.83
NO ₂	146.68 \pm 17.46	97.78 \pm 9.85	117.11 \pm 14.40	89.36 \pm 4.12	146.96 \pm 7.54
CO	1.47 \pm 0.32	1.36 \pm 0.51	1.23 \pm 0.51	0.97 \pm 0.22	0.83 \pm 0.26
NO	1.58 \pm 0.37	2.14 \pm 0.45	2.81 \pm 0.40	3.38 \pm 0.47	2.74 \pm 0.56

likely influenced by the topography and coastal meteorology (Abdulfattah *et al.*, 2025). Elevated concentrations of PM₁₀ and PM_{2.5} observed at L5 and L3 can be attributed to their proximity to vehicular access routes and construction-prone zones. Locations such as L1 situated closer to the sea front and adjacent to a green hill with greater exposure to breeze have recorded the lower mean concentrations and higher variability, thereby indicating the dispersive effect of coastal winds. L2 and L3 exhibited relatively higher levels of NO, NO₂, and SO₂, possibly due to localised anthropogenic emissions and restricted ventilation around the built-up areas. The observed standard deviations (Table 1) hint at the dynamic pollutant mixing influenced by land-sea interactions and diurnal shifts in boundary layer heights. Both the manual gravimetric sampling and continuous sensor-based monitoring were conducted during the study, and the close agreement between the two methods reinforces the reliability and accuracy of the measured pollutant concentrations.

While a vertical alteration in pollutant concentrations with increasing height is generally anticipated, this study quantifies the degree of that change and highlights its pollutant- and location-specific nature. PM_{2.5}, decreased by only 1.08% at L3 but dropped by over 10% at L2, suggesting localized atmospheric mixing suppression and continuous emissions at certain sites. PM₁₀ showed steeper variation (up to 15%), indicative of gravitational settling and coarse particle dominance. In contrast, gaseous pollutants like NO and CO exhibited more pronounced vertical gradients (25-35%), affirming their strong ground-level source signatures and limited dispersion under stable conditions. Notably, NO₂ and SO₂ displayed intermediate behaviour, with the change of 15-30%, suggesting combined surface emissions and some vertical transport or transformation. These variations underscore that vertical pollutant behaviour is not uniform and cannot be inferred from ground-level data alone. Moreover, coupling these profiles with meteorological stratification thresholds offers novel insight into how coastal atmospheric dynamics and emission source types shape vertical pollutant layering in dense urban environments.

Effect of vertical height on the pollutant dispersion

The distribution of the collected data for each of the five sampling locations is presented through box and whisker plots in Fig. 3. Particulate matter presented a more complex seasonal trend, with PM₁₀ concentrations exhibiting a significant vertical and seasonal gradient during summer, particularly at L1, L3, and L5, exceeding the NAAQM standards. High variability in PM₁₀ concentrations at lower heights also suggests transient dust episodes

from the construction activity adjacent to the locations and localized disturbances. On the Other hand, the PM_{2.5} has demonstrated a subtle seasonal pattern with concentrations being dominant in summer at L3 and L5, potentially due to dust resuspension, construction, and coastal salt transport (salt spray). All locations exhibited PM_{2.5} values well above the NAAQM limit of 60 $\mu\text{g m}^{-3}$, especially at lower altitudes. The vertical decline was consistently steep, with concentrations often halving from 0 m to 30-50m, consistent with gravitational settling and turbulence reduction with height (Gautam *et al.*, 2021; Hwang *et al.*, 2024).

SO₂ exhibited the most striking seasonal contrast among all pollutants. Winter concentrations at ground level were markedly higher, often approaching or surpassing the NAAQM threshold of 80 $\mu\text{g m}^{-3}$ at L1-L3. This may reflect increased emissions from fuel combustion as the parking slot being in proximity to the locations, coupled with limited vertical mixing during the winter seasons. The consistent decrease in SO₂ concentrations with height further reinforces its surface-bound emission signature. Notably, sites with broader interquartile ranges at lower heights suggest intermittent high-emission events, possibly linked to generator use or fuel combustion. NO₂, a secondary pollutant formed via atmospheric oxidation of NO, demonstrated both high baseline concentrations and notable exceedances of the NAAQM standard (80 $\mu\text{g m}^{-3}$), which may be attributed to its longer lifetime and partial contribution from aloft chemical transformations. Elevated wintertime NO₂ concentrations, peaking beyond 160 $\mu\text{g m}^{-3}$ at surface levels underscore the cumulative effect of restricted dispersion, high NO emissions, and suppressed photolytic breakdown due to reduced solar radiation (Horner *et al.*, 2024).

CO levels remained relatively low in summer across most locations, but in winter, elevated concentrations were consistently observed at ground level (0-10m), particularly at L3, L4, and L5, these seasonal peaks align with previously reported cold-seasonal accumulation due to reduced atmospheric mixing heights and increased combustion-related activities (Gautam *et al.*, 2021; Zheng *et al.*, 2023)we used an unmanned aerial vehicle associated with smart, low-cost sensors to record the vertical profiles of particulate matters (PM10/PM2.5/PM1). The vertical decay of CO with increasing height supports a local, ground-based source signature, typical of low-reactivity gases with minimal secondary formation. NO concentrations also followed a winter-dominant trend, with prominent peaks at lower altitudes and progressive decline with height. The steeper gradients were seen at L3-L5, where land use and activity density are higher. In contrast, summer NO levels showed less vertical stratification, suggesting improved atmospheric mixing

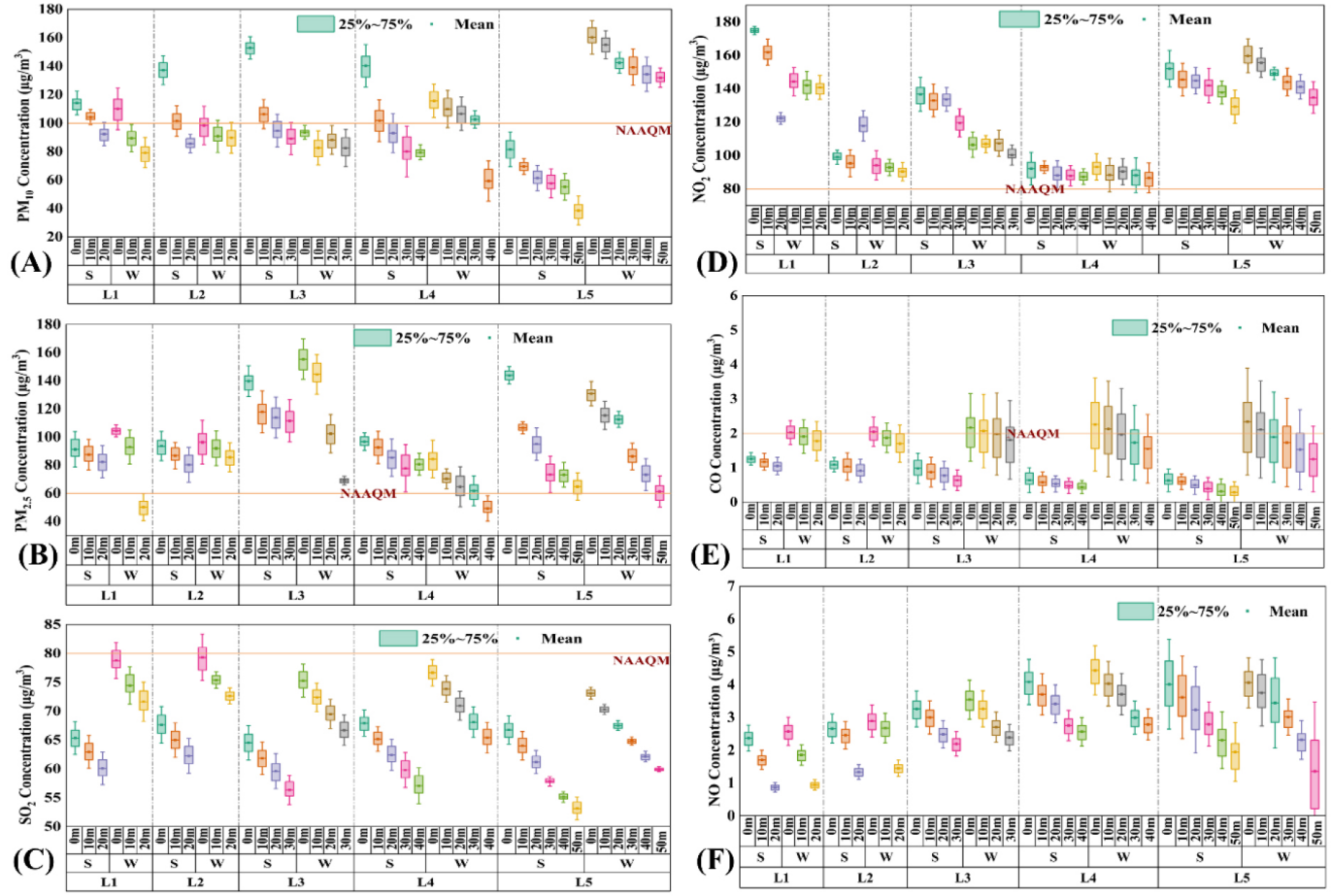


Fig. 3: Vertical and seasonal variations across locations (L1-L5): (A) PM_{10} , (B) $\text{PM}_{2.5}$, (C) SO_2 , (D) NO_2 , (E) CO , and (F) NO

under higher thermal turbulence.

Collectively, these box plot trends underscore that vertical heterogeneity in pollutant concentrations is governed not only by height but by seasonal meteorological conditions and emission characteristics. The direction of the exposure patterns resulted in showing the necessity of a multidisciplinary monitoring network that can help make safe and healthy levels. Additionally, the study highlights that there is an apparent correlation between the intensive industrial activities and high pollutant levels over L3-L5 areas, a stipulation that unventilated spaces with more pollution resources. The findings particularize the recent recommendations for pollution management strategies, localized and emphasizing both the vertical and the temporal variability of air pollutants (Priya and Iqbal, 2023).

Influence of meteorological parameters and height on the pollutant concentration

Variations in the concentration of the pollutants were investigated in this study in the five locations at different sampling show the effect of varied characteristics. The RH and temperature were measured in each trial at each of the specified heights for sampling. Considering the variations observed between the sampling locations, we infer that some of the influential factors that are specific to each sampling location are not captured in our study. Therefore, here we have analysed the role of RH, temperature,

and height in different sampling locations on the concentration of pollutants. To investigate the influence, the present study has employed Exhaustive CHAID (Chi-squared Automatic Interaction Detection) based decision tree (DT) models for the air pollutants.

The DT is a tree-like model with several layers of nodes, in which the first node is the root, the terminal nodes are the leaves, and the internal nodes between the root and the leaves correspond to specific attributes (Huynh-Cam *et al.*, 2021). In the present study, the independent models were constructed for every parameter using SPSS software, using height as the primary parameter to understand the heterogeneity in vertical dispersion and the identified threshold and dominant predictors from the CHAID model are shown in Table 2. The location and height have emerged as the critical dominants for the PM, while season and temperature for gaseous pollutants. PM_{10} found that the location is a dominant predictor with ($p < 0.001$), whereas L2 and L5 exhibited the highest baseline PM_{10} , with a mean of $101.31 \mu\text{g m}^{-3}$, and decreased with altitude to $64.34 \mu\text{g m}^{-3}$ at 40m, reinforcing the role of gravitational settling and emission (Cichowicz and Dobrzański, 2021) $\text{PM}_{2.5}$, $\text{PM}_{1.0}$, and hydrogen sulfide (H_2S).

For gaseous pollutants, the models revealed clear seasonal signatures. SO_2 and CO peaked in summer and winter respectively, reflecting the emission intensity and meteorological stability that

Table 2: Key predictors and threshold effects derived from CHAID decision tree models

Pollutant	Dominant Predictor	Secondary Predictors	Critical Thresholds / Key Findings	Interpretation
PM ₁₀	Location (p<0.001)	Height, Season, Temp	L2/L5: 101.3 $\mu\text{g m}^{-3}$ → 64.3 $\mu\text{g m}^{-3}$ at 40m; Temp 23.1–29.9°C → 138.2 $\mu\text{g m}^{-3}$	Site and height-dependent; thermal effects enhance mid-range values
PM _{2.5}	Height (p<0.001)	Location, RH, Temp	Ground: 110.9 $\mu\text{g m}^{-3}$ vs 63.0 $\mu\text{g m}^{-3}$ at 50m; >27.8°C and RH >70% → 137.8 $\mu\text{g m}^{-3}$	Strong vertical gradient; secondary formation intensified under warm-humid conditions
SO ₂	Season (p<0.001)	Height, Temp, RH	Summer peak: 112.2 $\mu\text{g m}^{-3}$; Height effect: 7.7 $\mu\text{g m}^{-3}$ (20 m) → 5.0 $\mu\text{g m}^{-3}$ (>45 m)	Seasonal dominance; vertical dilution reduces levels aloft
NO ₂	Temperature (p<0.001)	Height, Season	≤27.6°C: 141.8 $\mu\text{g m}^{-3}$ → >33.3°C: 174.9 $\mu\text{g m}^{-3}$; Ground: 165.3 $\mu\text{g m}^{-3}$ vs 138.9 $\mu\text{g m}^{-3}$ (30-40m)	Temperature-driven photochemistry; higher near surface due to emission proximity
CO	Season (p<0.001)	Location, Height, Temp	Winter: 1.93 $\mu\text{g m}^{-3}$ vs Summer: 0.88 $\mu\text{g m}^{-3}$; Ground: 0.58 $\mu\text{g m}^{-3}$ vs 0.33 $\mu\text{g m}^{-3}$ (>20m)	Strong seasonal dependence; accumulation under stable winter conditions
NO	Location (p<0.001)	Height, RH	L4 peak: 3.45 $\mu\text{g m}^{-3}$; Ground > elevated; RH >70% → 4.76 $\mu\text{g m}^{-3}$	Site-specific emission intensity; RH moderates atmospheric stability

hinders the dispersion. Further, the temperature played a key role in the dynamics of NO₂ pollutant as concentrations rising above 170 $\mu\text{g m}^{-3}$ at higher temperature thresholds due to enhanced photochemical activity. However, the concentrations of NO were primarily influenced by location, with the highest concentrations at L4 attributing to site-specific emission activity and limited dispersions.

Surface plot-based meteorological modulation of air pollutants

To understand the interactive effects of temperature and RH on the ambient concentrations of the studied pollutants, 3D surface plots were used as shown in Fig. 4. These visualizations have enabled a comprehensive interpretation of the meteorological modulations of the pollutant behaviour in the atmospheric boundary layer. The results clearly indicate the existence of the sensitivity of each pollutant to RH and temperature, which is similar in UAV-based vertical profiling and ground monitoring studies carried out in rural and peri-urban Indian locations. For PM₁₀, concentrations beyond 300 $\mu\text{g m}^{-3}$ are often observed in the middle range of the RH (55-70%) and moderately warm temperatures (26-30°C). A drop in PM₁₀ concentration was noticed at RH levels (RH < 50% and > 80%) shown in Fig. 4 (B), contributing to lesser surface area condensation and greater wet deposition. This seems to be in line with one of the urban micrometeorology studies, which suggests that RH seems to play the most dominant role in determining the PM concentration, and the temperature's effect on particle distribution seems much smaller than compared of the RH.

The 3D surface plot of PM_{2.5} shows the presence of high concentration values close to 600 $\mu\text{g m}^{-3}$ under air masses with moderate temperatures (26-28°C) and RH in the range of 70%-100% as shown in Fig. 4 (A). This result appears to imply that the growth and maturity of fine particulate matter tend to be more sensitive to the coupling of air temperature with humidity conditions, which plays a crucial role in particle resuspension, transformation processes (Bhatla *et al.*, 2025). The RH-induced hygroscopic growth of PM_{2.5} particulates accounts for the bulk of the mass enhancement,

in particular, during the warm and slightly humid conditions, and this is evident from the ongoing urban impacts of particulate matter (Ge *et al.*, 2021). Hygroscopic growth accounts for much of the mass increase, whereas sharp troughs at RH <50% and >85% indicate scavenging and limited nucleation. Concentrations drop significantly above 32°C, suggesting enhanced mixing and reduced particle residence times, as supported by thermodynamic principles.

The NO₂ surface plot depicts elevated concentrations (~200-300 $\mu\text{g m}^{-3}$) across moderate temperatures (26-32°C) and RH levels (60-80%), indicating its sensitivity to both primary emissions and photochemical formation (Abdulateef *et al.*, 2025). These results align with earlier studies highlighting RH's pivotal role in modulating NO₂ through chemical and physical pathways (Li *et al.*, 2024). These spikes can be caused by partial combustion of the fuel in industrial sources or vehicles, in which SO₂ oxidation does not occur. The process is hindered by the atmosphere being in a plume regime. Next, with a decile of RH >85%, a decline in SO₂ concentrations was also observed, an effect likely tied with the transformation of SO₂ in the aqueous phase to sulphate particles, and wet deposition (Chen *et al.*, 2022). The CO stationary concentration surface presented a rigorous single peak (~10 ppm) in a small amount of a RH ranging from 60 to 65% and a temperature of 25-28°C. Such conditions can thus favour the survival of CO in the atmosphere because of lower atmospheric shear and delayed combustion, especially when there is low wind or during early morning hours. The NO features a ridge of higher concentrations (~15 $\mu\text{g m}^{-3}$) at RH 60-70% and temperatures 26-30°C. This narrow window supports rapid chemical reactions where NO quickly oxidizes to NO₂. Increased concentrations at lower RH and higher temperatures (>30°C) suggest intensified vertical mixing, consistent with urban studies showing high spatiotemporal variability (Rajagopal *et al.*, 2025).

In summary, the surface plot analysis demonstrates that RH is more influential than temperature across pollutants in this coastal setting. Moderate RH promotes particulate growth, while extreme RH enhances deposition. Gaseous pollutants show

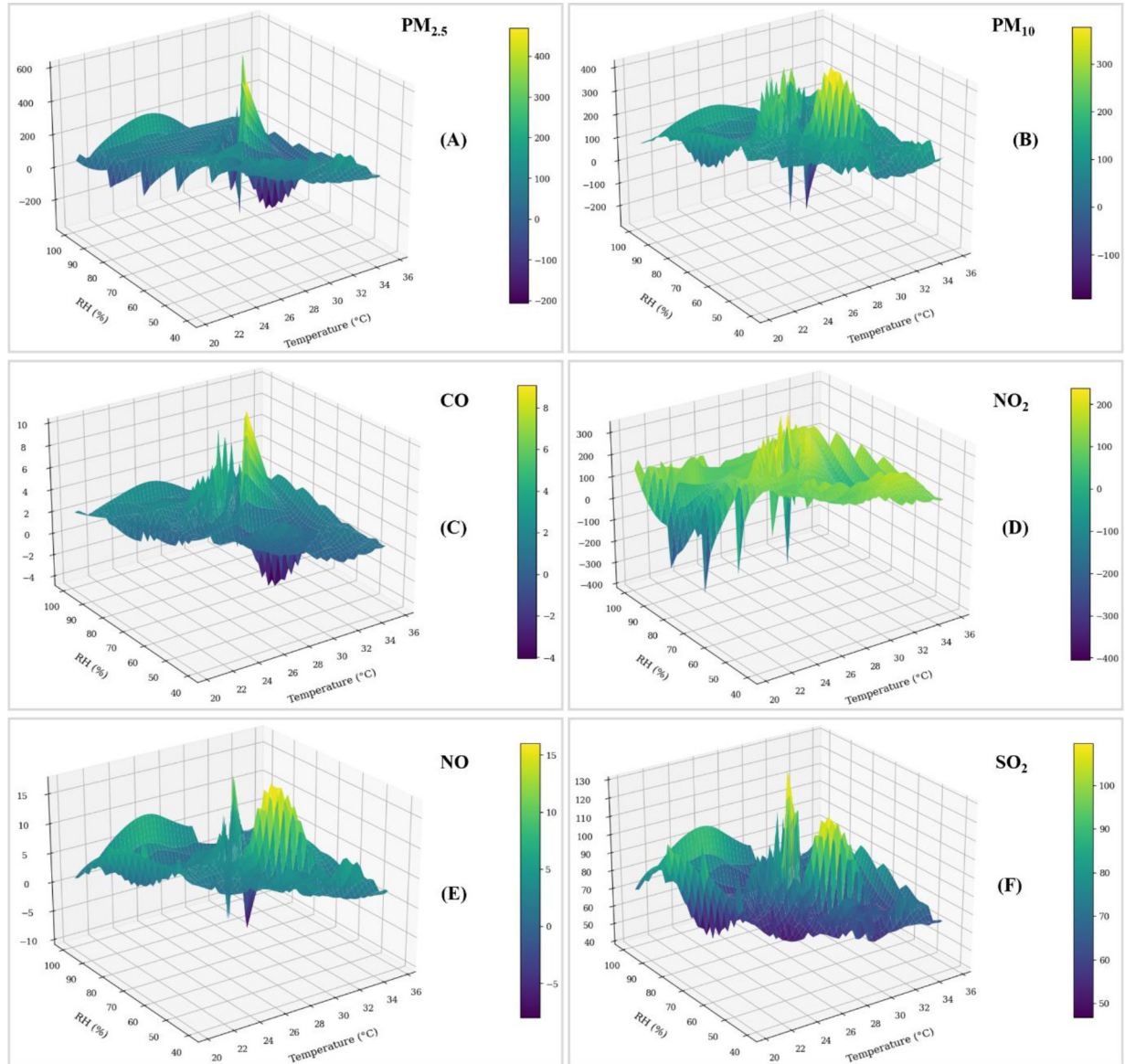


Fig. 4: Variation of pollutants with height and season across locations: (A) PM_{2.5}, (B) PM₁₀, (C) CO, (D) NO₂, (E) NO, and (F) SO₂

episodic peaks driven by RH-dependent chemical transformations and atmospheric stability. These results underscore the importance of high-resolution monitoring and meteorology-coupled modelling to better predict air quality fluctuations in humid coastal regions.

CONCLUSION

The present study has investigated the vertical distribution of air pollutants based on the measurements conducted using a stationary real-time multi-storey tower in an urban coastal city. Moreover, investigations were done during winters and summers in five different locations in Visakhapatnam, India, for PM₁₀, PM_{2.5}, CO, NO, NO₂, and SO₂, as well as temperature and relative humidity at different heights. Although wind speed is a dominant parameter in meteorological studies, owing to the defined scope and objectives, it was not considered in the current study. Considering this current limitation, future studies will aim to incorporate the wind speed to provide a comprehensive analysis.

The CHAID Algorithm was executed on the data collected, followed by an exhaustive decision tree model for all the pollutants analysed, and the thresholds derived, each of which posits a relationship between both location-specific factors and meteorological parameters. The findings indicate that meteorological conditions and altitude are specifically responsible for the formation and dispersion of pollutants. The winter atmospheric conditions caused strong downdrafts, which enhanced the vertical dispersion of pollutants at the surface. The whole scenario resulted in a pollution load. On another note, it was found that during the summer the dispersion conditions improved and the high temperature and humidity affected the pollution load. The seasonal stratification patterns and boundary layer interactions confirmed the findings, once again underscoring that coastal meteorology and urban morphology determine the mismatch of atmospheric pollutants. The study validates that the drivers of the vertical distribution of air pollutants not only depend upon the respective emission sources but also on the weather conditions that affect the structure of the

atmosphere.

The findings have significantly proved that the incorporation of integrated monitoring approach is required to better understand the variability of urban air quality. The study also emphasises that affiliating the vertical data with novel statistics is quintessential for understanding large scale pollution patterns, which are usually concealed in horizontal studies, further helping in supporting the necessary air quality management strategies.

ACKNOWLEDGEMENT

The authors sincerely acknowledge and thank the support provided by the MURTI Facility - GITAM (Deemed to be a university) and DST-FIST for providing facilities to carry out the work.

Funding: No funding was received for this work.

Availability of data: The author does not have permission to share the data used in this study.

Competing Interests: The authors have no relevant financial or non-financial interests to disclose.

Author Contributions: P.P. Nyayapathi: Study conception and design, Conceptualization, data curation, formal analysis, writing, review, and editing. N. Srinivas: Supervision and Conceptualization. S. K. Kollu: Conceptualization, review

Disclaimer: The contents, opinions, and views expressed in the research article published in the Journal of Agrometeorology are the views of the authors and do not necessarily reflect the views of the organizations they belong to.

Publisher's Note: The periodical remains neutral with regard to jurisdictional claims in published maps and institutional affiliations.

REFERENCES

- Abdulateef, Z. N., Talib, A. H., and Sultan, M. A. (2025). Spatiotemporal air quality variation between urban and agricultural areas: the influence of climatic factors and pollution dynamics. *J. Agrometeorol.*, 27(2):196-204. <https://doi.org/10.54386/jam.v27i2.2924>
- Abdulfattah, I. S., Rajab, J. M., Chaabane, M., and Lim, H. S. (2025). Trend analysis of air surface temperature using Mann-Kendall test and Sen's slope estimator in Tunisia. *J. Agrometeorol.*, 27(3):355-359. <https://doi.org/10.54386/jam.v27i3.3003>
- Bhatla, R., Raj, P., Kumar, P., Vishwakarma, A., and Dani, B. (2025). Spatio-temporal variations in air pollutants and their impact on wheat crop production in eastern Uttar Pradesh. *J. Agrometeorol.*, 27(2):148-156. <https://doi.org/10.54386/jam.v27i2.2862>
- Chen L-C, Maciejczyk P. D. and Thurston G. (2022). Chapter 6 - Metals and air pollution. In: Nordberg GF, Costa M (eds) Handbook on the Toxicology of Metals (Fifth Edition). Academic Press, pp 137-182
- Cichowicz R., and Dobrzański M. (2021). Spatial Analysis (Measurements at Heights of 10 m and 20 m above Ground Level) of the Concentrations of Particulate Matter (PM10, PM2.5, and PM1.0) and Gaseous Pollutants (H₂S) on the University Campus: A Case Study. *Atmos.*, 12:62. <https://doi.org/10.3390/atmos12010062>
- Gautam, S., Sammuel, C., Bhardwaj, A., Shams Esfandabadi, Z., Santosh, M., Gautam, A. S., Joshi, A., Justin, A., John Wessley, G. J., and James, E. J. (2021). Vertical profiling of atmospheric air pollutants in rural India: A case study on particulate matter (PM10/PM2.5/PM1), carbon dioxide, and formaldehyde. *Measurement*, 185: 110061. <https://doi.org/10.1016/j.measurement.2021.110061>
- Ge, W., Liu, J., Yi, K., Xu, J., Zhang, Y., Hu, X., Ma, J., Wang, X., Wan, Y., Hu, J., Zhang, Z., Wang, X., and Tao, S. (2021). Influence of atmospheric in-cloud aqueous-phase chemistry on the global simulation of SO₂ in CESM2. *Atmos. Chem. Phys.*, 21(21), 16093–16120. <https://doi.org/10.5194/acp-21-16093-2021>
- Gupta S., and Kumar R. (2023). Urban Areas and Air Pollution: Causes, Concerns, and Mitigation. In: Mushtaq F, Farooq M, Mukherjee AB, Ghosh Nee Lala M (eds) Geospatial Analytics for Environmental Pollution Modeling: Analysis, Control and Management. Springer Nature Switzerland, Cham, pp 163-185
- Horner RP, Marais EA, Wei N, Robert G. Ryan, and Viral Shah (2024). Vertical profiles of global tropospheric nitrogen dioxide (NO₂) obtained by cloud slicing the TROPOspheric Monitoring Instrument (TROPOMI). *Atmos. Chem. Phys.*, 24:13047-13064. <https://doi.org/10.5194/acp-24-13047-2024>
- Huynh-Cam T-T, Chen L-S, and Le H (2021) Using Decision Trees and Random Forest Algorithms to Predict and Determine Factors Contributing to First-Year University Students' Learning Performance. *Algorithms*, 14:318. <https://doi.org/10.3390/a14110318>
- Hwang, H., Lee, J. E., Shin, S. A., You, C. R., Shin, S. H., Park, J.-S., and Lee, J. Y. (2024). Vertical Profiles of PM_{2.5} and O₃ Measured Using an Unmanned Aerial Vehicle (UAV) and Their Relationships with Synoptic- and Local-Scale Air Movements. *Remote Sens.*, 16:1581. <https://doi.org/10.3390/rs16091581>
- Jalali Farahani, V., Altuwayjiri, A., Pirhadi, M., Verma, V., Alberto Ruprecht, A., Diapouli, E., Eleftheriadis, K., and Sioutas, C. (2022). The oxidative potential of particulate matter (PM) in different regions around the world and its relation to air pollution sources. *Environ. Sci. Atmos.*, 2:1076-1086. <https://doi.org/10.1039/D2EA00043A>

- Li, L., Li, J., Zhang, X., Lin, Y., Wang, R., Cao, J., and Han, Y. (2024). Effects of relative humidity on atmospheric organosulfur species derived from photooxidation and nocturnal chemistry in a forest environment. *Environ. Poll.*, 363: 125253. <https://doi.org/10.1016/j.envpol.2024.125253>
- Meo, S. A., Salih, M. A., Al-Hussain, F., Alkhalifah, J. M., Meo, A. S., and Akram, A. (2024). Environmental pollutants PM2.5, PM10, carbon monoxide (CO), nitrogen dioxide (NO_2), sulfur dioxide (SO_2), and ozone (O_3) impair human cognitive functions. *European Rev. Med. Pharmacol. Sci.*, 28(2): 789-796. https://doi.org/10.26355/eurrev_202401_35079
- Priya S., and Iqbal J. (2023). Assessment of NO_2 concentrations over industrial state Jharkhand, at the time frame of pre, concurrent, and post-COVID-19 lockdown along with the meteorological behaviour: an overview from satellite and ground approaches. *Environ. Sci. Poll. Res. Int.*, 30:68591-68608. <https://doi.org/10.1007/s11356-023-1975-8>
- 023-27236-2
- Rajagopal, K., Ramachandran, S., and Mishra, R. K. (2025). Influence of local meteorology and gaseous pollutant emissions on atmospheric nanoparticle concentrations in a pedestrian way in urban region. *Atmos. Poll. Res.*, 16:102358. <https://doi.org/10.1016/j.apr.2024.102358>
- Zhao, Y., Zhang, X., Chen, M., Gao, S., and Li, R. (2022). Regional variation of urban air quality in China and its dominant factors. *J. Geog. Sci.*, 32(5): 853-872. <https://doi.org/10.1007/s11442-022-1975-8>
- Zheng, Y., Li, W., Fang, C., Feng, B., Zhong, Q., and Zhang, D. (2023). Investigating the Impact of Weather Conditions on Urban Heat Island Development in the Subtropical City of Hong Kong. *Atmos.*, 14(2): Article 2. <https://doi.org/10.3390/atmos14020257>